

Contents

	Page
List of Figures	v
List of Abbreviations	vii
1. Primitives	1
1.1. PWM Loop	1
A. Comparator	1
B. Pulse-Width Modulator	3
C. PWM Loops	6
D. Offsets	7
E. Design Notes	9
1.2. Hysteretic Loop	10
A. Hysteretic Comparator	10
B. Hysteretic Loops	10
C. Offsets	11
D. Oscillating Period	14
E. Response Time (Bandwidth)	15
F. Design Notes	16
2. Summing Contractions	17
2.1. Summing Comparator	17
2.2. PWM Contractions	18
A. Voltage Loop	18
B. Current Loop	19
C. Current-Mode Voltage Loop	19
D. Offsets	20
2.3. Hysteretic Contraction	22
A. Current-Mode Voltage Loop	22
B. Offset	23
2.4. Load Compensation	24
2.5. Design Notes	26
3. Constant-Time Loops	26
3.1. SR Flip Flop	26
3.2. Pulse Generator	27
A. Set-Enabled	27
B. Reset-Enabled	28
3.3. Constant On Time	28
A. Current Loop	28
B. Offsets	29
C. Response Time	30
3.4. Constant Off Time	31
A. Current Loop	31

B. Offsets	32
C. Response Time	33
3.5. Constant Period	33
A. Current Loop	33
B. Sub-Harmonic Oscillation	34
C. Slope Compensation	35
D. Offsets	36
3.6. Design Notes	38
4. Oscillating Voltage-Mode Bucks	38
4.1. Resistive Capacitor	38
A. Output Voltage	38
B. Comparator Loops	39
C. Oscillating Period	40
D. Offsets	41
4.2. RC Filter	42
A. Comparator Loops	42
B. Oscillating Period	43
C. Offsets	43
D. Voltage-Mode Voltage Loop	45
4.3. Design Notes	47
5. Summary	47

List of Figures

	Page
Figure 1. Comparator.	1
Figure 2. Propagation delay.	2
Figure 3. Step response.	3
Figure 4. Pulse-width modulator.	4
Figure 5. Static PWM translation.	4
Figure 6. Dynamic PWM translation.	4
Figure 7. Inverting PWM translation.	5
Figure 8. PWM voltage loop.	6
Figure 9. PWM current loop.	7
Figure 10. PWM current-mode voltage loop.	7
Figure 11. Hysteretic comparator.	10
Figure 12. Hysteretic current loop.	10
Figure 13. Nominal hysteretic oscillation.	11
Figure 14. Hysteretic current-mode voltage loop.	11
Figure 15. Actual hysteretic oscillation.	11
Figure 16. Hysteretic response.	15
Figure 17. Summing comparator.	17
Figure 18. Summing equivalents.	18
Figure 19. Contracted PWM voltage loop.	18
Figure 20. Contracted PWM current loop.	19
Figure 21. Contracted PWM current-mode voltage loop.	19
Figure 22. Doubly-contracted PWM current-mode voltage loop.	20
Figure 23. Compact PWM current-mode voltage loop.	20
Figure 24. Contracted hysteretic current-mode voltage loop.	22
Figure 25. Load compensation.	24
Figure 26. Load-compensated PWM current-mode voltage loop.	25
Figure 27. Load-compensated hysteretic current-mode voltage loop.	25
Figure 28. SR flip flop.	26
Figure 29. Set-enabled pulse generator.	27
Figure 30. Reset-enabled pulse generator.	28
Figure 31. Constant on-time current loop.	29
Figure 32. Constant on-time oscillation.	29
Figure 33. Constant on-time response.	31
Figure 34. Constant off-time current loop.	31

Figure 35. Constant off-time oscillation.	32
Figure 36. Constant off-time response.	33
Figure 37. Peak current loop.	34
Figure 38. Valley current loop.	34
Figure 39. Sub-harmonic oscillation.	35
Figure 40. Slope compensation.	35
Figure 41. Slope-compensated peak current loop.	36
Figure 42. Buck output.	39
Figure 43. Resistive voltage-mode buck.	40
Figure 44. Filtered voltage-mode buck.	42
Figure 45. Filtered voltage-mode buck with resistive inductor.	44
Figure 46. Voltage-mode voltage-looped buck.	45

Switched Inductors: Control Loops

Switched-inductor (SL) power supplies normally close feedback loops that sense the output, amplify the error, and adjust inductor current so the error is low. With this feedback action, they can feed any current the load or controller demands. This is how *voltage regulators*, *battery chargers*, and *light-emitting diode (LED) drivers* supply power.

Perhaps the most distinguishing feature in their implementations is how the error adjusts the inductor current. In this respect, although often described in unique and stand-alone terms, most switched-inductor power-supply systems evolve from two basic primitives. Variations on these then germinate features and restrictions that ultimately set them apart.

1. Primitives

1.1. PWM Loop

A. Comparator

A *comparator* compares two analog voltages and outputs a digital voltage to indicate which is higher. The *output* v_O reaches the *output high* V_{OH} in Fig. 1 when the *positive input* v_P surpasses the *negative input* v_N and the *output low* V_{OL} when v_N exceeds v_P . In CMOS implementations, V_{OH} and V_{OL} are usually the *positive* and *negative power supplies* v_{DD} and v_{SS} .

The *differential input voltage* v_{ID} is the difference between v_P and v_N . From this perspective, v_O reaches V_{OH} when v_{ID} is positive and V_{OL} when v_{ID} is negative. Comparators therefore dual as *polarity detectors*.

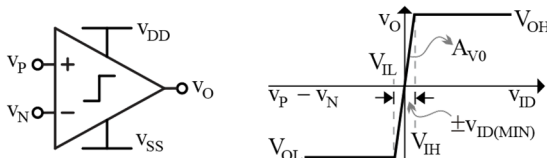


Fig. 1. Comparator.

Solution:

$$\Delta v_S = v_{S(HI)} - v_{S(LO)} = 500\text{m} - 200\text{m} = 300\text{ mV}$$

$$v_I = v_{S(LO)} + \Delta v_S d_o = 200\text{m} + (300\text{m})(45\%) = 340\text{ mV}$$

$$v_I = v_{S(HI)} - \Delta v_S d_o = 500\text{m} - (300\text{m})(45\%) = 360\text{ mV}$$

$$d_{o(MIN)} = \frac{t_p}{t_{CLK}} = \frac{100\text{n}}{1\mu} = 10\%$$

C. PWM Loops

The *PWM voltage loop* in Fig. 8 is the classic *PWM voltage-mode regulator*. CP_{PWM} and v_S translate the *amplified error voltage* v_{EO} into the *energize duty-cycle command* d_E' that energizes the *switched inductor* L_X . f_{CLK} determines the *switching frequency* and *period* f_{sw} and t_{sw} of L_X .

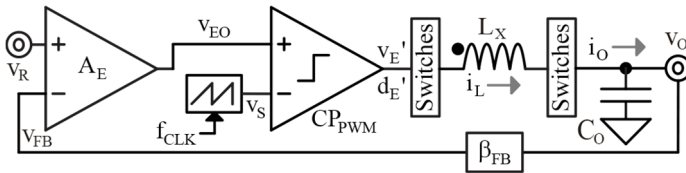


Fig. 8. PWM voltage loop.

The *feedback translation* β_{FB} scales v_O to the *feedback voltage* v_{FB} that the *error amplifier* A_E compares to the *reference voltage* v_R . So A_E outputs the v_{EO} that sets and adjusts d_E' so L_X 's *inductor current* i_L supplies the *output current* i_O needed to keep the error low. This way, v_{FB} nears v_R and v_O is close to a reverse β_{FB} translation of v_R .

The *PWM current loop* in Fig. 9 is a direct translation of the voltage loop in Fig. 8. This loop senses and regulates i_L or i_O . So the error that feeds CP_{PWM} and adjusts d_E' is the *current-error voltage* v_{IO} .

The *current-feedback translation* β_{IFB} scales i_L or i_O to the *current-feedback voltage* v_{IFB} that the *current-error amplifier* A_{IE} compares to the *current-reference voltage* v_{IR} . A_{IE} outputs the v_{IO} that sets and adjusts d_E'

1.2. Hysteretic Loop

A. Hysteretic Comparator

The *hysteretic comparator* CP_{HYS} in Fig. 11 is a comparator that decouples and shifts v_{ID} 's *rising* and *falling* trip points $v_{T(HI)}$ and $v_{T(LO)}$. This way, v_O rises to V_{OH} after v_{ID} rises over $v_{T(HI)}$ and falls to V_{OL} after v_{ID} falls under $v_{T(LO)}$. But v_O does not trip when v_{ID} rises over $v_{T(LO)}$ or when v_{ID} falls below $v_{T(HI)}$. The difference between these trip-points is the *hysteresis* Δv_T .

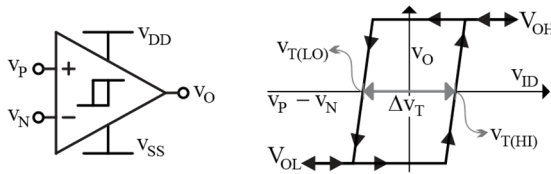


Fig. 11. Hysteretic comparator.

v_N 's trip points oppose v_P 's in v_{ID} . This is because v_O trips low when v_N rises $-v_{T(LO)}$ over v_P and trips high when v_N falls $-v_{T(HI)}$ below v_P . This is like saying v_N 's $v_{T(HI)}$ and $v_{T(LO)}$ are v_P 's $-v_{T(LO)}$ and $-v_{T(HI)}$.

B. Hysteretic Loops

The *hysteretic current loop* in Fig. 12 is a *relaxation oscillator* that centers on the hysteretic comparator and slewing action of i_L . β_{IFB} is usually a resistor that converts i_L to v_{IFB} . This way, v_{IFB} rises and falls with i_L .

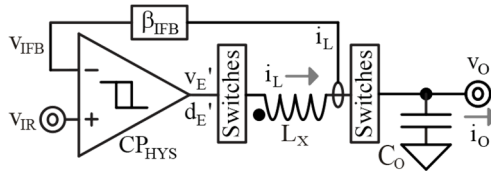


Fig. 12. Hysteretic current loop.

CP_{HYS} waits for the v_E the switcher impresses across L_X to slew i_L and v_{IFB} high to v_{IFB} 's $v_{T(HI)}$ in Fig. 13. When v_{IFB} overcomes $v_{T(HI)}$, CP_{HYS} trips $v_{E'}$ low. This prompts the switcher to apply v_D across L_X , which slews i_L down. CP_{HYS} "relaxes" as i_L slews down, until v_{IFB} reaches v_{IFB} 's $v_{T(LO)}$. At this point, CP_{HYS} trips high and v_{IFB} 's $i_L\beta_{IFB}$ again climbs towards $v_{T(HI)}$.

$$\begin{aligned}\Sigma v_{ID} &= v_{EO} - v_{IFB} - v_S = (v_R - v_{FB})A_E - v_{IFB} - v_S \Big|_{A_E=1} \\ &= v_R - v_{FB} - v_{IFB} - v_S = v_R + (-v_S) - v_{FB} - v_{IFB}\end{aligned}\quad (34)$$

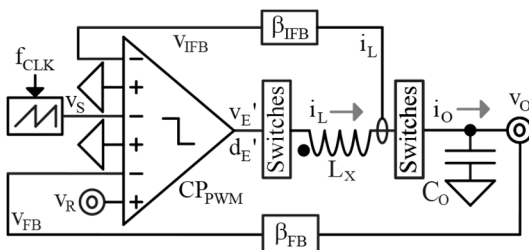


Fig. 22. Doubly-contracted PWM current-mode voltage loop.

This is like subtracting v_{FB} and v_{IFB} from v_R and $-v_S$. With v_S inverted this way, Σv_{ID} adds two v_P 's and two v_N 's like CP_{PWM} in Fig. 23. Either way, incorporating A_E and A_{IE} into CP_{PWM} is a *double contraction*.

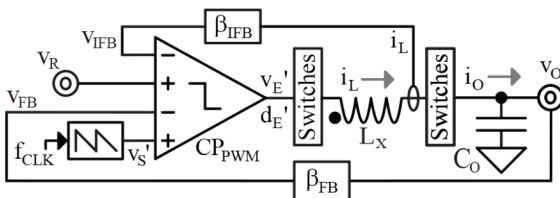


Fig. 23. Compact PWM current-mode voltage loop.

These double contractions are stable without z_{DO} when the *capacitor pole* p_C that C_O produces reduces A_{LG} to f_{0dB} at or below the *current loop's bandwidth* p_{IBW} that the *current loop's unity-gain frequency* f_{0dB} sets. It is also stable when the roles of p_C and p_{IBW} reverse. p_C and p_{IBW} can also precede f_{0dB} when z_C reverses p_C at or below f_{0dB} . With z_{DO} , stable operating conditions are more elusive.

D. Offsets

The v_{IOS} needed to set $d_{E'}$ is a $d_{E'}$ fraction of Δv_S over $v_{S(LO)}$. Since this v_{IOS} is a v_P in Σv_{ID} and v_{IR} minus v_{IFB} generates v_{IOS} , v_{IFB} is v_{IOS} below v_{IR} . v_{FB} in the PWM voltage loop is similarly v_{IOS} below v_R :

$$v_{IOS} = v_{S(LO)} + \Delta v_S d_{E'} \quad (35)$$

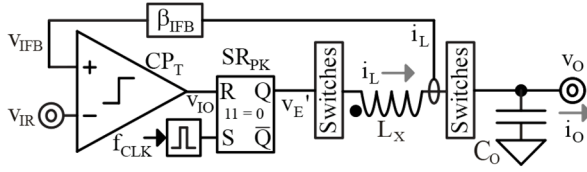


Fig. 37. Peak current loop.

t_R^+ is also the same. When v_{IR} rises suddenly, v_{IR} surpasses v_{IFB} , so v_{IO} falls and stays low. This raises and keeps $v_{E'}$ high because, once f_{CLK} sets $v_{E'}$, subsequent lows keep $v_{E'}$ high. So i_L rises uninterruptedly across t_R^+ .

t_R^- , however, is shorter. When v_{IR} falls suddenly, v_{IR} falls below v_{IFB} , so v_{IO} rises and stays high. This keeps $v_{E'}$ low because the *peak flip flop* SR_{PK} is reset-dominant. This way, i_L falls uninterruptedly across t_R^- .

The *valley current loop* in Fig. 38 is the peak's complement. CP_T starts t_E when v_{IFB} falls below v_{IR} , v_{IFB} rises until f_{CLK} ends t_E , and $v_{E'}$ stays low and high with v_{IO} across t_R 's. So v_{IR} sets $v_{IFB(LO)}$, t_{CLK} fixes t_{SW} , and i_L rises and falls across t_R^+ and t_R^- without interruptions.

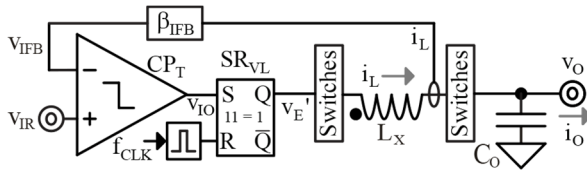


Fig. 38. Valley current loop.

B. Sub-Harmonic Oscillation

v_{IN} noise can change the di_L/dt that projects i_L across $\Delta v_{IFB}/\beta_{IFB}$, which can alter t_E or t_D . A temporary rise in $v_{E'}$'s v_{IN} , for example, raises di_L^+/dt in Fig. 39. So i_L reaches v_{IR}/β_{IFB} sooner, falls across a longer t_D , and reaches di_{L0} below the nominal $i_{L(LO)}$.

di_{L0} extends the next t_E that di_L^+/dt projects. This shortens t_D because t_{SW} is constant. So di_L^-/dt projects i_L above the nominal $i_{L(LO)}$. Since dE/dD is $v_D/v_{E'}$, the new imbalance di_{L1} is an inverting dE/dD translation of di_{L0} :

Slope compensation adds another *offset* v_{SOS} . v_S subtracts a d_E fraction of Δv_S from $v_{S(HI)}$ or adds a d_E fraction of Δv_S over $v_{S(LO)}$. So in all, v_{IOS} is

$$v_{IOS} = \frac{\Delta v_{IFB}}{2} - v_{IOS}^+ + v_{SOS} = \frac{\Delta v_{IFB}}{2} - v_{IOS}^+ \pm (v_{S(LO/HI)} \pm \Delta v_S d_E'). \quad (63)$$

Example 12: Determine $v_{S(HI)}$, Δv_{IFB} , v_{EO} , and v_{FB} for the peak current-mode voltage loop when v_R is 1.2 V, A_E is 10 V/V, β_{IFB} is 1 Ω , t_{CLK} is 1 μs , t_p is 100 ns, t_{SR} is 10 ns, $v_{S(LO)}$ is 200 mV, v_E is 2.2 V, v_D is 1.8 V, L_X is 10 μH , and $i_{L(AVG)}$ is 100–500 mA.

Solution:

$$\Delta v_S = t_{CLK} \left(\frac{dv_{IFB}}{dt} \right) \equiv t_{CLK} \left(\frac{0.5v_D}{L_X} \right) = 90 \text{ mV}$$

$$v_{S(HI)} = v_{S(LO)} + \Delta v_S = 200\text{m} + 90\text{m} = 290 \text{ mV}$$

$$d_E = \frac{v_D}{v_E + v_D} = \frac{1.8}{2.2 + 1.8} = 45\%$$

$$t_E = t_{CLK} d_E = (1\mu)(45\%) = 450 \text{ ns}$$

$$\Delta v_{IFB} = t_E \left(\frac{v_E}{L_X} \right) \beta_{IFB} = (450\text{n}) \left(\frac{2.2}{10\mu} \right) (1) = 99 \text{ mV}$$

$$t_p' = t_p + t_{SR} = 100\text{n} + 10\text{n} = 110 \text{ ns}$$

$$\begin{aligned} v_{IOS} &= \frac{\Delta v_{IFB}}{2} - t_p' \left(\frac{v_E}{L_X} \right) \beta_{IFB} + v_{S(LO)} + d_E \Delta v_S \\ &= \frac{99\text{m}}{2} - (110\text{n}) \left(\frac{2.2}{10\mu} \right) (1) + 200\text{m} + (45\%)(90\text{m}) \\ &= 270 \text{ mV} \end{aligned}$$

$$v_{EO} = i_{L(AVG)} \beta_{IFB} + v_{IOS} = i_{L(AVG)} + 270 \text{ mV} = 570 \pm 200 \text{ mV}$$

$$v_{FB} = v_R - \frac{v_{EO}}{A_E} = 1.2 - \frac{v_{EO}}{10} = 1.14 \text{ V} \pm 20 \text{ mV}$$

$$\begin{aligned} \therefore \Delta v_{FB} &\approx \Delta v_T + t_p \left(\frac{v_E + v_D}{R_F C_F} \right) \beta_{FB} = 41 \text{ mV} \\ &= \Delta v_T + \frac{(100n)(2.2+1.8)(66\%)}{(800k)(20p)} \rightarrow \Delta v_T = 24 \text{ mV} \end{aligned}$$

$$\Delta v_F = \frac{\Delta v_{FB}}{\beta_{FB}} = \frac{41m}{66\%} = 62 \text{ mV}$$

$$t_E = d_E t_{SW} = \left(\frac{v_D}{v_E + v_D} \right) t_{SW} = \left(\frac{1.8}{2.2+1.8} \right) (1\mu) = 450 \text{ ns}$$

$$\begin{aligned} \Delta v_O &\approx \frac{v_E t_E^2 + v_D t_D^2}{8L_X C_O} \approx \frac{v_E t_E^2 + v_D (t_{SW} - t_E)^2}{8L_X C_O} \\ &= \frac{(2.2)(450n)^2 + (1.8)(1\mu - 450n)^2}{8(10\mu)(5\mu)} = 2.5 \text{ mV} \end{aligned}$$

Note: Δv_O is much lower than Δv_F .

D. Voltage-Mode Voltage Loop

The *voltage-mode voltage-looped buck* in Fig. 46 uses the filtered buck like a current loop. This way, β_{FB2} scales v_O to v_{FB2} , A_{E2} compares v_{FB2} to v_R , and the filtered buck translates v_{EO2} to $i_{L(AVG)}$. So v_{EO2} adjusts the $i_{L(AVG)}$ that sets i_O so v_{FB2} and v_O near v_R and v_R/β_{FB2} .

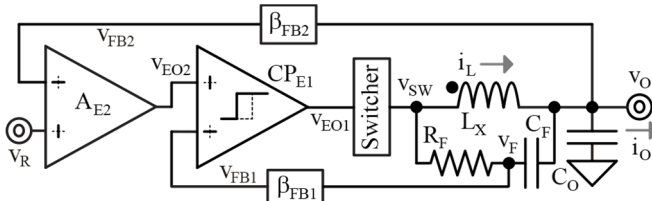


Fig. 46. Voltage-mode voltage-looped buck.

v_{FB2} and v_{EO2} are steady because C_O suppresses v_O 's ripple. CP_{E1} , however, needs this v_{EO2} to carry a β_{FB1} translation of $v_{F(AVG)}$. v_R minus